Highway Visibility Detection Using Hough Circle Detection and Incremental Probabilistic Neural Networks

Yun Tan
Hunan Xiangjian Zhike Engineering Technology Co., Ltd. Changsha 410000, China
Email of: tanyunxjzk@126.com

Keywords: hough circle detection algorithm, incremental probabilistic neural network, highway pavement, visibility

Received: July 2, 2024

In traditional highway engineering, there are problems such as high cost and difficult maintenance in road visibility detection. Therefore, the study combines Hough circle detection algorithm with incremental probabilistic neural network to construct a visibility detection model for highway pavement. The study first uses the Hough circle detection algorithm to perform preliminary visibility detection, and then integrates the incremental probabilistic neural network with the preliminary detection to construct a detection model. These results confirm that the data processing accuracy and precision of the detection model in the image processing process are 97.03% and 93.37%, respectively. In terms of feature classification performance, its classification ability and classification time are 93.61% and 1.13 seconds, respectively. Moreover, its visibility and error percentage in visibility detection are 510.69 m and 10.06%, respectively. Regardless of the weather conditions, the environmental classification accuracy of the model remains above 90%, with the highest accuracy reaching 93.7% for sunny days. These results indicate that the highway pavement visibility detection model can improve the accuracy and stability of highway pavement visibility detection. The research aims to provide an effective visibility detection method for highway traffic safety.

Povzetek: Razvit je bil model za zaznavanje vidljivosti cestne površine, ki združuje algoritem zaznavanja krogov Hough in inkrementalno probabilistično nevronsko mrežo (IPNN). Model dosega dobro zaznavanje v različnih vremenskih pogojih, kar izboljšuje varnost cestnega prometa.

1 Introduction

Highway engineering includes roadbed, pavement, bridges, culverts, tunnels, drainage systems, safety protection facilities, etc. Among them, road surface visibility in highway engineering is an important research direction for traffic safety. Visibility refers to the degree to which the driver of a vehicle can clearly see the road ahead under different weather conditions while driving [1-3]. The visibility is closely related to the incidence of traffic accidents, and its main detection methods include instruments and images currently. Due to the high cost and difficulty of instrument detection equipment, research is being conducted on using image processing technology combined with deep learning algorithms to detect the visibility of road surfaces. To ensure the standardization of visibility detection, the study refers to the "Visibility Observation Specification" of the Meteorological Detection Center of China Meteorological Administration as the technical guidance document for visibility detection, thus ensuring the scientific nature of visibility detection. The Hough circle detection algorithm can detect geometric shapes such as lines and circles in images, but its processing effect on blurred images is poor. Incremental Probabilistic Neural Network (IPNN) has adaptive learning ability, which can automatically adjust network parameters and improve detection accuracy [4-6]. Therefore, the study fuses Hough with IPNN to construct a Highway Payment Visibility Detection (HPVD) model. The study first uses Hough to detect road visibility, and then introduces IPNNs to combine their advantages for constructing a detection model. The research innovatively combines the Hough algorithm with IPNNs, fully utilizing the respective advantages of both. The visibility detection model integrating Hough algorithm and IPNN not only makes full use of the advantages of image processing technology, but also introduces the powerful ability of deep learning, which can significantly improve the accuracy and reliability of visibility detection in highway engineering. At the same time, the application of Hough algorithm and IPNN in road engineering visibility detection research is still in the primary stage. How to further optimize the network structure, improve the detection speed, enhance the anti-jamming ability, etc., are the important direction of future research. The research aims to use the constructed HPVD to improve the accuracy of visibility detection and provide new ideas and methods for ensuring highway traffic safety.

The study first uses Hough to conduct preliminary detection of road surface visibility. Then, based on Hough visibility detection, it is fused with IPNN to construct HPVD. The third part verifies the performance of the constructed model for comment classification through

simulation experiments and practical applications. Finally, the experimental results are summarized, and the advantages and disadvantages of the research methods are analyzed.

2 Related works

In recent years, HPVD has received widespread attention. Traditional HPVD has many issues, such as accuracy, real-time performance, range coverage, cost, and maintenance. To address these issues, researchers have begun exploring image processing-based HPVD. Meng and Wu proposed an HPVD method to enhance HPVD. This method performed grayscale processing on the collected images, then utilized adaptive steering filtering algorithm and quadtree image segmentation algorithm for processing, and finally calculated visibility based on the offset of distances in the images. These results confirmed that image processing methods optimized through visibility detection could address low image clarity, color distortion, and poor scene adaptability [7]. Ma et al. proposed a hybrid model for analyzing road line of sight using airborne LiDAR data to apply high-density LiDAR to visibility detection along highways. In the study, triangulation was used to collect and analyze data, and then a backpropagation network was used to train these data. These results confirmed that the computational efficiency of the hybrid model in estimating line of sight had been improved to a satisfactory level [8]. Ashrit established a high-resolution visibility detection model to improve the predictive ability of road visibility under dense fog. The study first graded visibility, and then used models with different resolutions for prediction. These results confirmed that the real-time aerosol field in the model could further improve the prediction of visibility by high-resolution models [9]. Ding et al. proposed a comprehensive optimization control method to improve the safety and traffic efficiency of visibility areas on highways. The study first involved discrete queuing of vehicles at upstream intersections, followed by trajectory optimization. These results confirmed that it could not only prevent trajectory overlap, but also effectively reduce road traffic delays [10].

Ma et al. proposed an accurate and effective obstacle framework to ensure the safety of highway traffic. The study first used mobile laser scanning data to scan highways, and then analyzed and processed the scanning data. These results confirmed that the framework could detect visual obstacles at each viewpoint on the highway within 0.2 seconds [11]. Ismail et al. to effectively detect defects in composite structures, the defect factors of cylinders with different layup angles were analyzed using finite element analysis. The study utilized sensitivity analysis to analyze the defect factors and the results showed that the results by finite element analysis coincided with the results of critical buckling load. The study helped to determine the parameters that lead to the defect tolerance of the structure [12]. Easa et al. proposed a new LiDAR 3D surveying system to apply ranging systems to highway design. This system could effectively detect obstacles by utilizing infrastructure and high-precision maps. These results confirmed that this method could effectively improve the estimation of traffic visibility and location recognition [13]. To conduct effective research on the application of IPNN in artificial intelligence accelerators, Banerjee et al. used a bottom-up approach for the first time to systematically describe the impact of this uncertainty and imprecision (collectively referred to as defects) in IPNN. These results confirmed that the inference accuracy of IPNN also slightly decreased, and the inference accuracy was sensitive to defects in the linear layer next to the input layer of IPNN [14]. The summary table for related works is shown in Table 1.

Table 1: Summary table for related works

Researchers	Method	Research results	Disadvantages
Meng and Wu [7]	Enhanced HPVD	Solve the problems of low image definition, low color distortion and poor scene adaptability	High computational complexity
Ma et al. [8]	Hybrid model	Calculation efficiency reaches 91%	There may be a risk of overfitting in the model
Ashrit [9]	High-resolution visibility detection model	The accuracy of visibility prediction reaches 90%	Poor model interpretability
Ding et al. [10]	Comprehensive optimization of the control method	Effectively reduce road traffic delays	Greatly affected by the environment
Ma et al. [11]	The obstacle frame	Detected obstacles within 0.2 seconds	There are issues such as false positives and missed detections
Ismail et al. [12]	A sensitivity analysis was used to analyze the defect factors	Help to determine the parameters that lead to the tolerance of the structural	The analysis process is complex

		defects	
Easa et al. [13]	Lidar 3D measurement system	Improve estimates of traffic visibility and location identification	High equipment cost
Banerjee et al. [14]	The bottom-up approach systematically describes the impact of defects in IPNN	The inference accuracy is sensitive to defects in the linear layer next to the input layer of IPNN	The detection and repair process is quite complex

In summary, the research on visibility detection in highway engineering based on image processing technology combined with deep learning is very important. Although this technology has achieved certain results in improving visibility detection accuracy, real-time performance, and range coverage, there are still some problems that need to be solved, such as low image clarity, color distortion, and poor scene adaptability. In addition, there is still a need for in-depth research on visibility prediction under dense fog conditions, safety of visibility areas on highways, and optimization of traffic efficiency. To better address these issues, research has achieved the detection of road visibility by effectively integrating Hough and IPNN, providing a more accurate road visibility assessment method for traffic safety.

3 Design of a highway pavement visibility detection model that integrates hough and IPNN

With the development of computer vision and image processing technology, image processing-based HPVD has become a hot research topic. The fusion of Hough and IPNN in HPVD has significant research value.

3.1 Road visibility detection based on hough

To effectively detect visibility in road surfaces, effective image processing is required after collecting video images. Image processing can eliminate noise interference, improve the acquisition of target feature area feature values, and improve the accuracy of road visibility detection. The research first performs grayscale processing on the image to reduce the computational complexity of image processing. The images in the video are all composed of static images, so it is necessary to process a certain frame of the video image. In this study, three colors of red, green, and blue are used to construct image pixel channel components [15-16]. A gray image is a single-channel mean obtained by weighting three channel components. This processing not only greatly reduces the computational complexity of the image, but also ensures that there is only a color difference from the original image. The weighted mean of the processed image pixels is represented by Eq. (1).

$$f(i,j)=0.3R(i,j)+0.59G(i,j)+0.11B(i,j) \quad (1)$$

In Eq. (1), $R(i,j)$ represents the weighted mean of red flux. $0.59G(i,j)$ represents the weighted mean of green flux. $0.11B(i,j)$ represents the weighted mean of blue flux. After completing the grayscale processing of the image, it is necessary to filter the image. The main function of filtering is to better suppress image noise while ensuring the detailed features of the image. The study analyzes a large number of image processing literature and uses median filtering method to filter images. It belongs to nonlinear filtering technology, which can effectively suppress nonlinear noise during the process of filtering images. It can also replace the pixels in the image with the median of all pixels in the filtering window. At this point, the corresponding two-dimensional median filter can be represented by Eq. (2).

$$g(i,j)=med(f(i-k,j-l)) \quad (2)$$

In Eq. (2), $g(i,j)$ represents the filtered output image. $f(i,j)$ is the input value before filtering. k and l belong to the templates in two-dimensional filtering, both of which are odd numbers. Median filtering requires effective processing of the original pixel length and filtering template to complete sorting and obtain the filtered results when processing images. After completing the filtering operation on the image, it is necessary to effectively extract the feature values of the feature regions in the image. In the study, Hough circle detection algorithm is used to locate image features and improve image processing capabilities. By studying the processing of Hough circle detection algorithm in images, traditional Hough circle detection algorithms are easily affected by environmental factors during the processing. It requires a large amount of computation, which leads to a decrease in accuracy during processing. Therefore, gradient region growth is introduced in the Hough circle detection algorithm. Gradient growth can aggregate pixels with consistent gradients, thereby reducing the impact of noise on image circular segments and improving the accuracy and reliability of detecting target circular regions [17-18]. Fig. 1 shows the Hough circle image detection flowchart for gradient region growth. The Hough circle detection

algorithm is a commonly used image processing method for detecting circular objects in images. This algorithm is based on the gradient information of the image. By calculating the gradient direction of pixels in the image, it locates the regions of different arcs and finds circular objects. In the gradient region growth stage, the algorithm first finds pixels with the same gradient direction, which are located at the edges of the image features. To determine these regions, the algorithm needs to utilize the linear regions in the image. Specifically, the algorithm defines the gradient variance between two adjacent pixels on a straight line in a linear region. By calculating the gradient direction difference, it can find the most suitable pixel set and fit different types of arc segments. At this stage, the algorithm will determine which pixels should be included in the circle based on the magnitude and direction of the gradient variance. Generally speaking, pixels with smaller gradient variances are more likely to be located at the edges of a circle, while pixels with larger gradient variances are more likely to be located at the center of the circle. Therefore, the algorithm will first select pixels with small gradient variance as candidate points for the circle, and then fit the equation of the circle based on the positions and gradient directions of these points. The gradient direction difference can be represented by Eq. (3).

$$\tau = \left| d_1(x_1, y_1) - d_2(x_2, y_2) \right| < \frac{2\pi}{n} \tag{3}$$

In Eq. (3), τ represents the gradient direction difference. $d_1(x_1, y_1)$ represents the

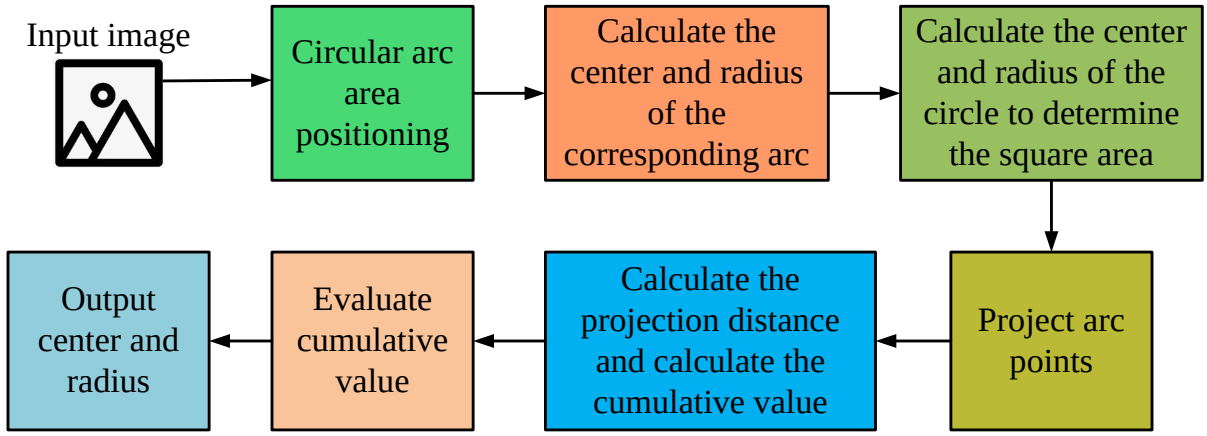

Figure 1: Flow chart of Hough circle image detection for gradient region growth

coordinate point of the first pixel. $d_2(x_2, y_2)$ represents the coordinate point of the second pixel. n represents directional accuracy. After obtaining the fitted arc segment through gradient direction difference, the observation image can be calculated. At this point, the image can be represented by Eq. (4).

$$\Delta J = \Delta I + \Delta\omega \tag{4}$$

In Eq. (4), ΔI represents the image value without noise. $\Delta\omega$ represents the quantization error value between two adjacent pixels. Fig. 2 is a schematic diagram of the relationship between directional angle and noise quantization during image processing to determine the pixel error caused by noise. After obtaining the relationship between the two, the study also needs to calculate the values of the arc and the center and radius of the processed circle in the image processing process. By finding any three coordinate points on an arc, the center and radius of the circle can be calculated, which can be represented by Eq. (5).

$$\begin{cases} (x_1 - a)^2 + (y_1 - b)^2 = r^2 \\ (x_2 - a)^2 + (y_2 - b)^2 = r^2 \\ (x_3 - a)^2 + (y_3 - b)^2 = r^2 \end{cases} \tag{5}$$

In Eq. (5), a and b represent the center value of the circle. After calculating the center value and radius, the projection distance in the image can be calculated and statistically analyzed. By calculating the projection distance, the position and size of the object in the image can be evaluated. The projection distance here is represented by Euclidean distance using Eq. (6).

$$D(i, j) = \sqrt{(x_i - x_j)^2 + (y_i - y_j)^2} \tag{6}$$

In Eq. (6), (x_i, y_i) represents any coordinate point in the arc. (x_j, y_j) represents any coordinate point in the

positive direction region.

3.2 Construction of visibility detection model using hough combined with IPNN

After using gradient region growth Hough for grayscale and image processing, it is possible to evaluate the position and size of objects in the image. After completing the evaluation, it is also necessary to classify visibility based on the information of the object to complete the detection of visibility in the road surface. Therefore, it is necessary to establish a classification of visibility based on the feature information in road surface images and road visibility. IPNN is applied in the road visibility detection. IPNN is based on probability theory, which combines the advantages of probability theory and neural networks, and continuously optimizes the network parameters through incremental learning to achieve accurate processing of complex data. In IPNN, each neuron has probabilistic outputs, and these probabilistic outputs reflect the neuron's confidence in the input data. In highway engineering visibility detection, IPNN can effectively deal with various uncertainties and noise disturbances to improve the accuracy and robustness of detection. By introducing probabilistic output, IPNN can automatically adjust the connection weights between neurons to adapt to different input data. This incremental learning property enables the IPNN to continuously learn from new data and improve its performance, thus realizing accurate visibility detection. After setting the expected value, when the training error is greater than the expected value, the network can improve the training intensity by increasing the number of hidden layer neurons until the required error requirements are obtained, thereby completing the detection of road visibility [19-20]. Fig. 3 shows the structure of IPNN.

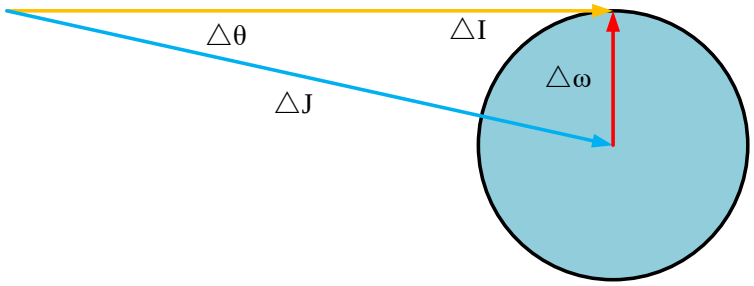

Figure 2: Schematic diagram of the relationship between directional angle and noise quantization in image processing

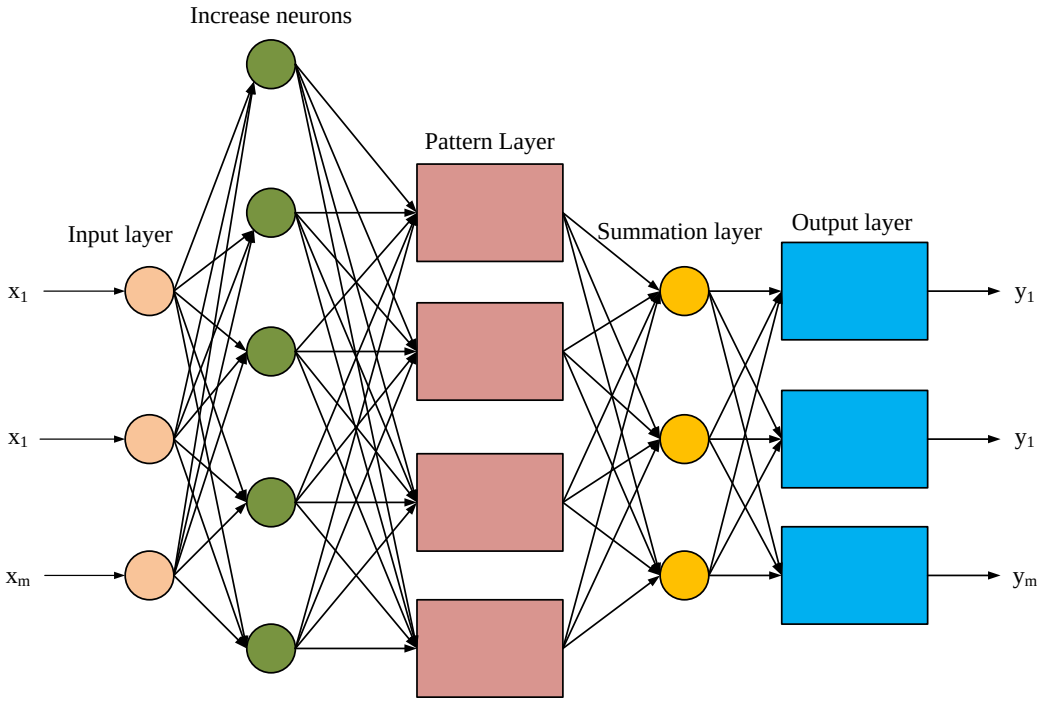

Figure 3: Schematic diagram of the structure of IPNN

In Fig. 3, when using IPNN for training, it is necessary to construct a radial base layer and an output layer. The radial base layer can initialize threshold and weight values. When the training results do not meet the expected values, it can act as a hidden layer to learn and extract useful features from the input data to update the threshold. By updating the threshold, the training error can be optimized to meet the expected value. Next is the construction of the output layer, which can be represented by Eq. (7).

$$T = \max(wa^1) \tag{7}$$

In Eq. (7), T represents the target vector. w represents the image output weight. a^1 is the output of the radial base layer. After completing the construction of the radial base layer and output layer, the neural network in IPNN can be optimized to calculate the error between the actual and output values, which can be calculated using Eq. (8).

$$err = \sum_{j=1}^{k} (a_j^3 - t_j)^2 \tag{8}$$

In Eq. (8), a_j^3 represents the actual output value. t_j indicates the target output value. The accuracy of training results can be improved through the increase of neurons, but the structure of neural network has also become complex. The complex structure will increase the time-consuming in the training process, and also affect the accuracy of the data. The smoothing factor is included in the radial base constructed in the study. The smoothing factor plays a role in controlling the complexity of the model, affecting the learning performance and determining the size of the basis function in IPNN. By adjusting the smoothing factor reasonably, the learning performance and generalization ability of IPNN can be optimized. This shows that the size of smoothness factor will directly affect the complexity of IPNN in visibility detection of road image [21]. Therefore, it is necessary to select an appropriate smoothing factor to reduce the complexity of neural network in the process of operation. To obtain a more balanced smoothing factor, Particle Swarm Optimization (PSO) is used to optimize the smoothing factor of IPNN. When optimizing the smoothing factor, it is necessary to initialize the parameters of PSO. Fig. 4 is the flow chart of PSO optimizing IPNN. In Fig. 4, on the basis of setting parameters, it is also necessary to select the fitness function to find the optimal position of particles through iteration. At this time, the fitness function can be expressed by Eq. (9).

$$F_i = \left| \frac{a_i^3 - T_i}{T_i} \right| \tag{9}$$

In Eq. (9), a_i^3 is the number of the i-th particle before optimization. T_i represents the difference between the actual outputs. By calculating the fitness function, the optimal position of the particle swarm can be calculated. After obtaining the optimal position of the particle swarm, it is also necessary to pay attention to the update speed and position information of the particles at any time. The update speed here can be calculated by Eq. (10).

$$V_{i,d}^{t+1} = w \times v_{i,d}^t + Q_i \times (pbest_{i,d}^t - x_{i,d}^t) + c \times rand \times (gbest_{g,d}^t - x_{i,d}^t) \tag{10}$$

In Eq. (10), $V_{i,d}^{t+1}$ represents the updated speed. w is the weight value of inertia. $v_{i,d}^t$ is the speed that is not updated. Q_i means speed control factor. $pbest_{i,d}^t$ indicates the optimal position of the current particle search. $x_{i,d}^t$ is the position before the update. c is the learning factor. $gbest_{g,d}^t$ indicates the optimal position searched by the current particle swarm. The updated location information can be expressed by Eq. (11).

$$x_{i,d}^{t+1} = x_{i,d}^t \times Q_i + V_{i,d}^{t+1} \tag{11}$$

In Eq. (11), $x_{i,d}^{t+1}$ represents the updated position. After obtaining the updated velocity and position information, the diversity scale of particle swarm can be defined. The determination of diversity scale can update the optimal value of individual particles to obtain the optimal value of particle swarm. At this time, the position update can be expressed by Eq. (12).

$$x_{i,d} = \begin{cases} P_{g,d} + 0.01 \times rand(1, D) & rand < r \\ P_{g,d} & otherwise \end{cases} \tag{12}$$

In Eq. (12), $P_{g,d}$ means the local optimal position. $rand(1, D)$ is a random number between [0, 1]. r represents the pulse frequency value emitted in the process of particle optimization. By judging the position and the number of new iterations, if all the optimal positions have been found, the optimal solution will be output, and the value of the optimal solution can be used as the smoothing factor of IPNN. The pseudocode for IPNN training is shown in Figure 5.

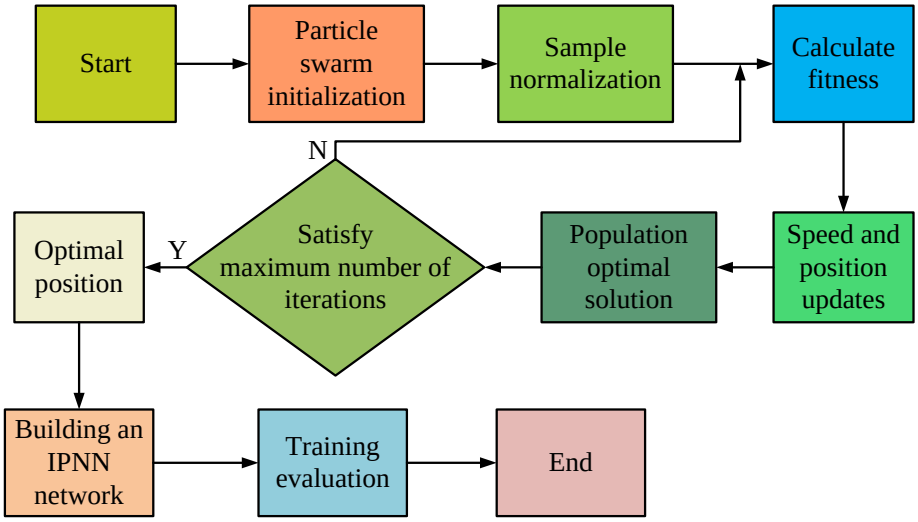

Figure 4: Flowchart of particle swarm optimization for IPNN

```
IPNN_Training():
    initialize_radial_basis_layer_threshold_and_weight()
    while (training_result_not_expected):
        update_threshold_as_hidden_layer()
        optimize_training_error()
    construct_output_layer()
    initialize_particle_swarm_optimization_parameters()
    select_fitness_function()
    while (not_converged):
        best_position = calculate_fitness_function()
        updated_speed = calculate_speed_update()
        updated_position = calculate_position_update()
        define_diversity_scale()
        if (found_optimal_position):
            output_optimal_solution_as_smoothing_factor()
    return classification_result
```

Figure 5: Flow chart of highway pavement visibility detection using Hough algorithm combined with IPNN

In summary, through image processing and feature extraction, the collected image information to be measured is input into the model for training, and the classification results of highway pavement visibility are obtained. Fig. 6 shows the flow chart of HPVD based on Hough and IPNN.

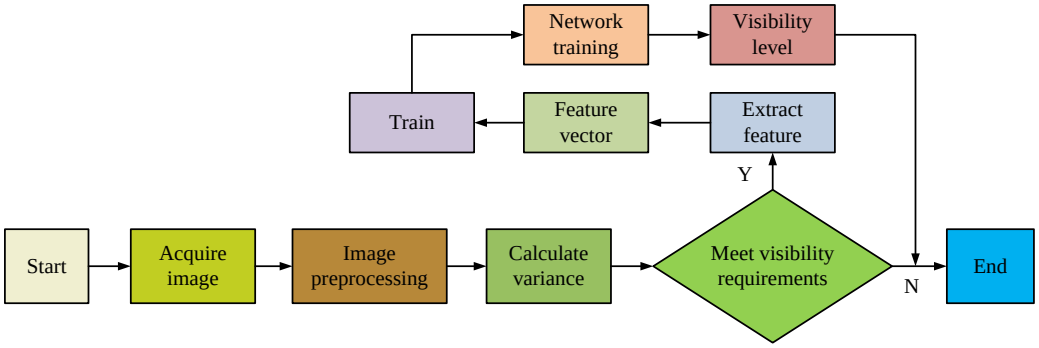

Figure 6: Flow chart of highway pavement visibility detection using Hough algorithm combined with IPNN

4 Performance analysis of visibility detection model for highway pavement

To verify the performance of HPVD, according to the relevant national standards, combined with the actual situation of calculation, pavement visibility was divided into six cases. The study collected 150 groups of experimental samples through authorization, covering 6 kinds of road visibility. The collected experimental samples were used to construct the data set, and the data set was used to verify the performance of the model.

4.1 Performance analysis of visibility detection model

The hardware configuration used in the experiment was a laptop equipped with a Core i5-8250U processor and a memory configuration of 16 GB. The operating system selected was Windows 10, and the development environment adopted Anaconda 4 distribution, which had rich built-in Python libraries and tools.

To verify the performance of HPVD, the study first verified the grayscale processing effect of the model. Images collected at 10, 20, 50, 100, 500, and 1000 meters were used as conditions for grayscale processing, and the performance of the model was reflected based on the grayscale processing results of images at different distances. Fig. 7 shows the average grayscale and distortion of color blocks under typical visibility.

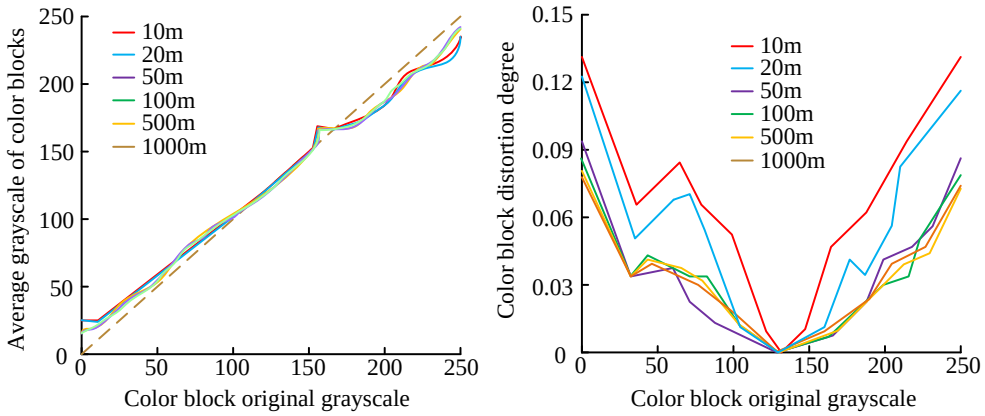

(a) Mean grayscale variation of color blocks under typical visibility

(b) Color block distortion at typical visibility distances

Figure 7: Mean grayscale and distortion of color blocks under typical visibility

According to Fig. 7(a), as the average grayscale of the color block changed, there were some fluctuations in the average grayscale of the color block as the distance increased. The large grayscale variation of the color blocks indicated low visibility, which was significantly related to weather and air quality. According to Fig. 7(b), as the original grayscale and visibility distance of the color block increased, the distortion of the color block showed a trend of first decreasing and then increasing. This indicated a monotonically decreasing relationship between the degree of distortion of color block images and the distance of visibility. Besides, the color block distortion in the study had a certain degree of symmetry, which also indicated that the prediction model constructed in the study had good image grayscale processing ability. To verify the performance of the model in image processing, a comparison was conducted between the dark primary color prior algorithm, dual brightness difference method, and detection model. The comparison indicators were the accuracy and precision of image processing. Fig. 8 shows the comparison results of image processing accuracy and precision among three methods. According to Fig. 8(a), the image processing accuracy of all three methods was at a high level. The data processing accuracy of the detection model in the image processing process was 97.03%. The data processing accuracy of the prior algorithm for dark primary color and the double brightness difference method were 92.11% and 89.54%, respectively. In Fig. 8(b), the difference in precision among the three methods during image processing increased. The precision of the detection model in the image processing process was 93.37%. The processing precision of the prior algorithm for dark primary color and the double brightness difference method were 88.92% and 82.69%, respectively. This indicates that the visibility detection model constructed in the study has better robustness in image processing. To verify the feature classification and detection efficiency of the detection model in visibility images, the feature classification performance and time consumption were used as indicators. Fig. 9 shows the comparison of feature classification performance and classification time of three methods.

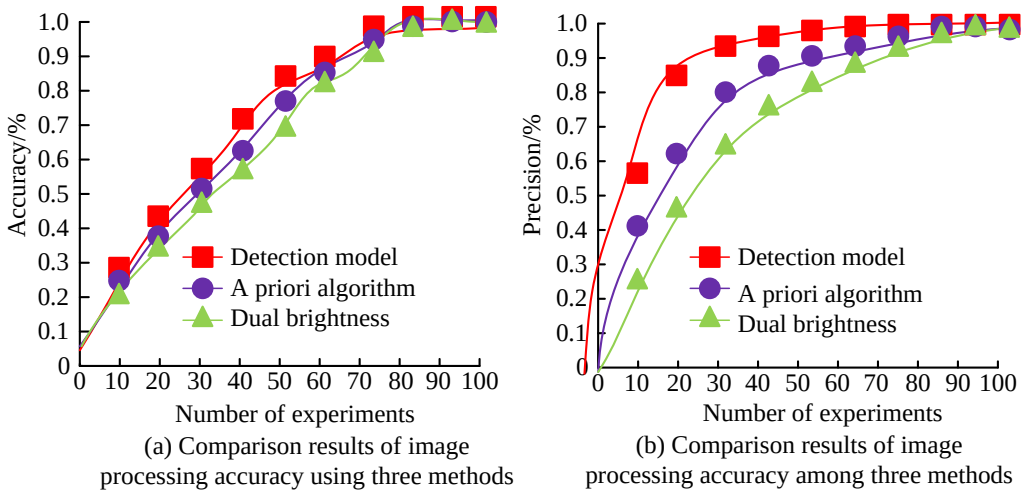

(a) Comparison results of image processing accuracy using three methods

(b) Comparison results of image processing accuracy among three methods

Figure 8: Comparison of accuracy and precision of image processing using three methods

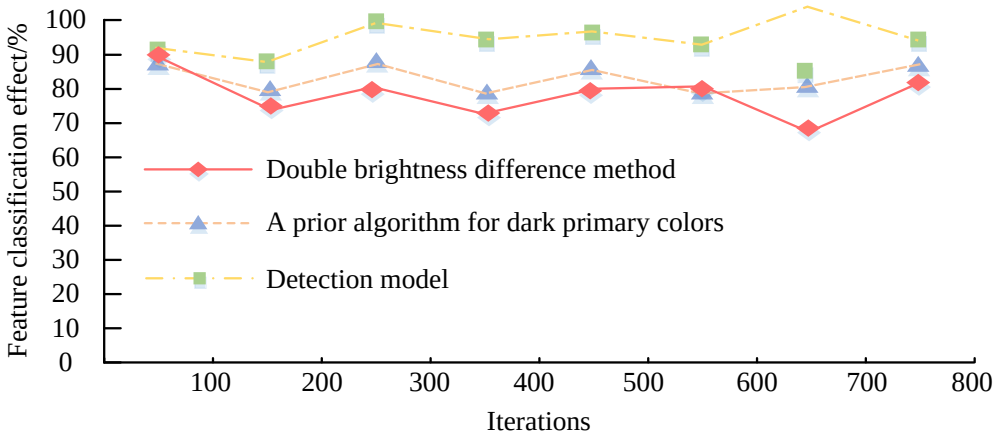

(a) The feature classification performance of three methods

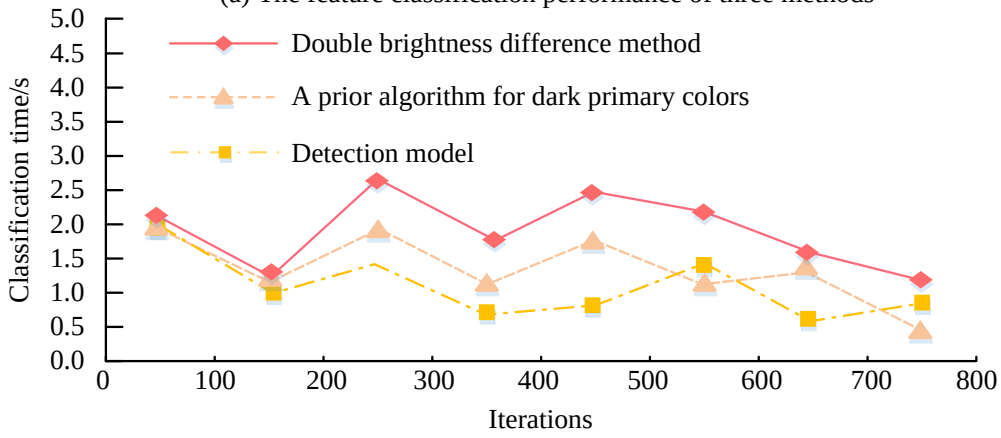

(b) The classification time of three methods

Figure 9: Comparison of feature classification performance and time of three methods

According to Fig. 9(a), the dual brightness difference method had the worst classification performance in feature classification of visibility images, while the detection model had the best performance. The feature classification

performance of this detection model reached 93.61%. The image feature classification performance of the dark primary color prior algorithm and the dual brightness difference method were 86.73% and 81.29%, respectively. According to Fig. 9(b), the feature classification time of the detection model was 1.13 s. The classification time of the dark primary color prior algorithm and the dual brightness difference method were 1.96 s and 2.49 s, respectively. This indicates that the detection model can have better recognition performance in a shorter time. To further verify the effectiveness of the detection model in detecting visibility on highway pavements, the visibility detection results and detection error percentage of the three methods were used as indicators. Fig. 10 shows the comparison results of visibility detection and error percentage using three methods.

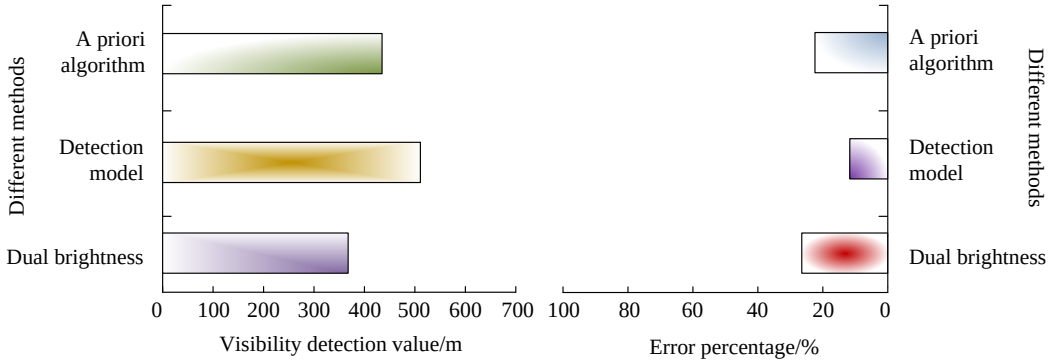

(a) Comparison results of visibility detection using three methods

(b) The percentage of detection error for three methods

Figure 10: Comparison results of visibility detection and error percentage using three methods

According to Fig. 10(a), there were significant differences in visibility detection among these three methods under the same weather conditions. The visibility of the detection model reached 510.69 m. The visibility detection values of the dark primary color prior algorithm and the dual brightness difference method were 426.59 m and 372.89 m, respectively. According to Fig. 10(b), there was also a significant difference in the percentage of error among these three methods. The visibility error percentage of the detection model was 10.06%. The visibility error percentages of the dark primary color prior algorithm and the dual brightness difference method were 17.93% and 23.91%, respectively. This indicates that the constructed HPVD has high adaptability in the visibility detection of highway pavement.

4.2 Application performance analysis of visibility detection model

To validate the application performance of HPVD, this study collected 150 sets of data as input. The data came from actual road monitoring equipment and meteorological station records. When using this data, 70% of it was used as the training set to train the detection model and enable it to learn the features and patterns in the data. The remaining 30% was be used as a test set to evaluate the performance of the detection model on new data and test its generalization ability. The study took the time consumption and visibility detection error of different visibility video sizes as indicators. Fig. 11 shows the time consumption, visibility recognition results, and error analysis of visibility recognition.

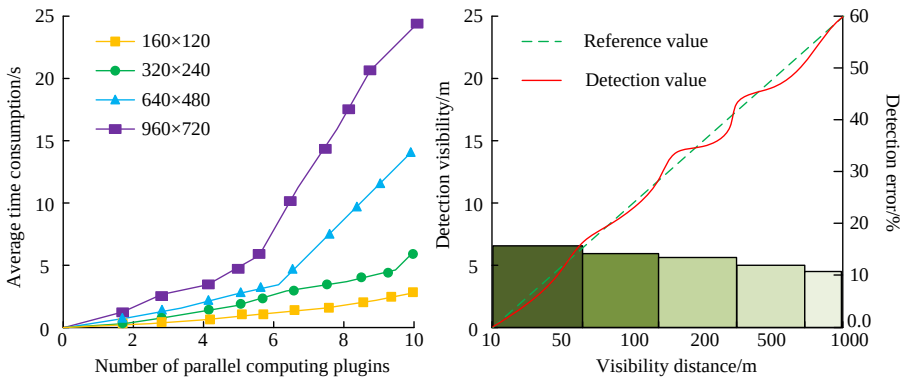

(a) Time consumption for visibility recognition of different video frame sizes

(b) Visibility results and error analysis

Figure 11: Time consumption, visible recognition results, and error analysis for visibility recognition

According to Fig. 11(a), as the number of video plugins increased, the average time consumption for different video frame sizes showed a significant increase. The larger the video frame, the more time it took. The average time consumption for video 160×120 was 3.2 s, 4.6 s for video 320×240, 7.2 s for video 640×480, and 13.9 s for video 960×720. This indicates that, while ensuring accurate visibility judgment, the video used for visibility analysis can be selected based on the size of the video frame. According to Fig. 11(b), as visibility increased, the detection error of visibility showed a decreasing trend. Although there was a certain difference between the visibility detection value and the visibility reference value, the general trend was the same. The detection error was 13.69% when the visibility was between 10 and 50 m, 11.27% between 50 and 100 m, 10.59% between 100 and 200 m, 10.12% between 200 and 500 m, and 10.03% between 500 and 1000 m. This indicates that the visibility detection model has high accuracy and effectiveness. To verify the detection performance of the detection model during the day and evening, the instrument detection results were compared with the detection model in the study. Fig. 12 shows the visibility detection results of two methods during the day and evening. According to Fig. 12(a), the difference between these two methods was not significant in the visibility detection of road surfaces during the day. The minimum and maximum visibility distribution detected by the instrument was [186.93 m, 1198.76 m], while the detection model was [183.57 m, 1183.26 m]. According to Fig. 12(b), in the detection of visibility on the evening road surface, the detection model was directly affected by light due to the collected videos for analysis, resulting in a significant decrease in the detection effect of visibility. At this point, the distribution of the minimum and maximum visibility values of the detection model was [139.58 m, 519.22 m]. Although the visibility detection model was affected to some extent in the evening, the visibility detection results it obtained still had reference value. To further validate the performance of the detection model, a 24-hour comparison was conducted between the predicted values of the detection model and the true values of visibility. Fig. 13 shows the comparison between the predicted values of the detection model and the actual values.

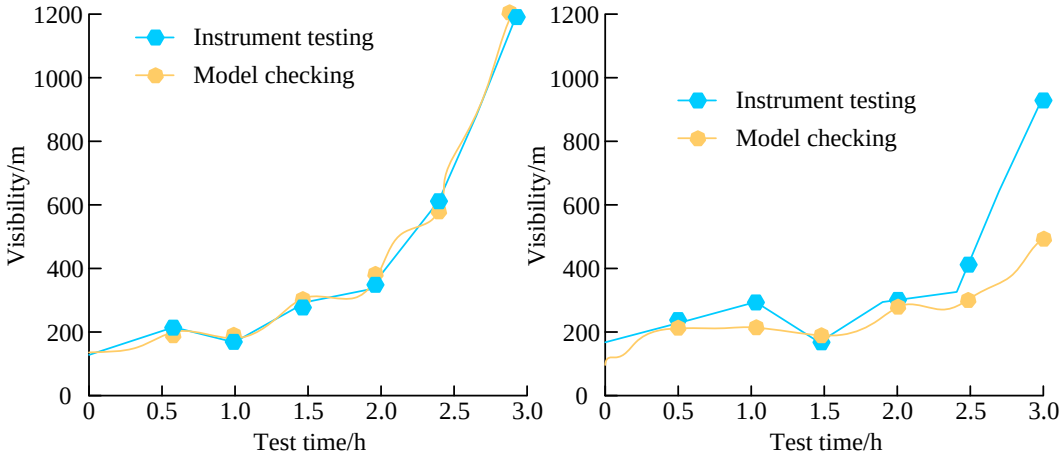

(a) Comparison of daytime test results between predictive models and instrument detection

(b) Comparison results between predictive models and instrument testing in the evening

Figure 12: The visibility detection results of two methods during the day and evening

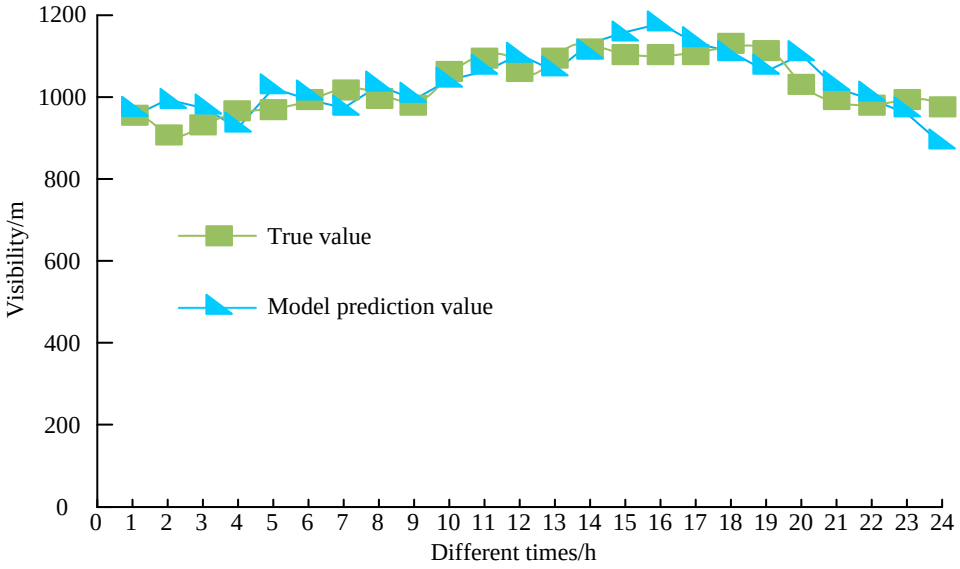

Figure 13: Comparison results between predicted and true values of the detection model

According to Fig. 13, the average visibility of the true values throughout the entire detection was 1098.35 m. There was a certain difference between the predicted values of the detection model and the true values of visibility, with an average visibility value of 1029.76 m. The comparison between the actual and predicted visibility values showed that the constructed highway pavement detection model had a certain degree of reliability and could be applied to the corresponding HPVD. To verify the effectiveness of the application of the visibility model, the study used the false alarm rate of the visibility detection model as a sensitivity detection index for exploring the sensitivity of the visibility detection model. The results of the false alarm comparison between the model and the traditional visibility detection method and the true value of visibility are shown in Fig. 14.

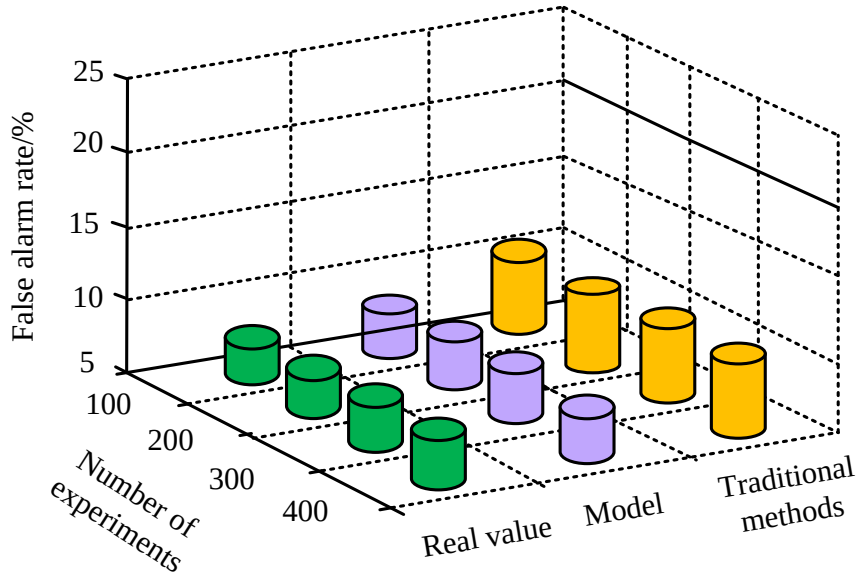

Figure 14: False alarm comparison results of the model with traditional visibility detection methods and true values of visibility

In Figure 14, in visibility sensitivity detection, the detection sensitivity false alarm rate of the traditional method was 10.53%. The visibility detection sensitivity false alarm rate of visibility detection model was 7.29% and the true false alarm rate of visibility was 6.08%. There was a difference of 4.45% and 1.21% between the sensitivity false alarm rate of the traditional method and the visibility detection model compared to the true value.

This indicates that the visibility detection model has a high detection sensitivity with a small difference from the true value. To further validate the performance of the visibility detection model, the study was conducted to measure the actual visibility, as shown in Fig. 15, which shows the results of the visibility image comparison before and after the visibility model processing. The comparative analysis of Fig. 15 shows that the visibility raw images were introduced into the visibility detection model and combined with the features of highway surveillance images. The study utilized the Hough algorithm for noise reduction and graying of the original image. Meanwhile, IPNN was utilized to increase the processing capacity of the neural network to ensure that the image visibility features are not lost during the refinement. Comparison of Fig. 15 (a) and (c) revealed that the gap between the refinement results and the real value was significantly reduced, which indicated that the visibility detection model had a stable and reliable performance in both visibility detection effect and real-time performance.

To verify the scalability and robustness of the proposed model, the experiment analyzed the accuracy, recall, F1 score, and AUC of the model under the Nighttime visibility dataset. The Nighttime visibility dataset includes visibility data under different weather conditions, road types, and vehicle speeds, with over 10000 observations. The scalability and robustness evaluation results of the model are shown in Table 2. In Table 2, the proposed model performed exceptionally well in various environments and conditions. Firstly, regardless of whether the weather conditions were sunny, cloudy, rainy, or snowy, the environmental classification accuracy of this model remained above 90%, with the highest classification accuracy of 93.7% for sunny days. This indicates that the model has good environmental adaptability and can accurately classify environments under various weather conditions. Whether it is dry, wet, waterlogged, or snowy roads, the classification accuracy of the model remained above 90%, with dry roads having the highest classification accuracy, reaching 94.3%. This indicates that the model has good robustness and can accurately classify environments under various road surface conditions. In the case of low-speed, medium-speed, and high-speed vehicles, the classification accuracy of the model was above 90%, with low-speed vehicles having the highest classification accuracy, reaching 95.3%. This indicates that the model has good speed adaptability and can accurately classify environments at various vehicle speeds. In summary, the proposed model has good scalability and robustness, and can accurately classify environments in various environments and conditions, which is of great significance for traffic safety applications.

(a) Original images (b) Initial processing of images (c) Model refinement of processed images

Figure 15: Comparison results of visibility images before and after visibility model processing

Table 2: Model scalability and robustness assess the knot

Environment	Classification	Accuracy	Recall	F1 score	AUC
Meteorological condition	Sunny	93.7%	91.3%	92.1%	0.91
	Cloudy	92.7%	90.3%	91.7%	0.89
	Rain	92.9%	91.3%	91.6%	0.90
	Snowy	92.1%	90.1%	90.3%	0.88
Road surface type	Dry	94.3%	91.7%	93.1%	0.92
	Damp	94.1%	90.3%	92.7%	0.90
	Accumulated water	91.5%	90.9%	91.2%	0.90
	Accumulated snow	90.1%	89.9%	90.0%	0.87
Vehicle speed	Low	95.3%	94.1%	94.8%	0.93
	Medium	94.3%	92.7%	93.9%	0.92
	High	93.7%	95.3%	94.6%	0.90

This study developed an HPVD for detecting visibility on highway surfaces. The results indicated that the model outperformed other methods in terms of accuracy and precision in visibility detection, and had a lower false alarm rate and good real-time performance. The constructed HPVD model had high reliability and practicality in road visibility detection. Compared with the research methods in related works, the visibility detection model proposed in the study had better performance in accuracy, precision, and real-time performance. This is because this study employed deep learning techniques to learn more complex and advanced feature representations, thereby improving the performance of the model. Compared to the hybrid model proposed by Ma et al., the visibility detection model proposed in this study used road monitoring video data, which had better stability and real-time performance. The proposed model can learn more complex and advanced feature representations in a unified model, thereby improving the performance of the model. However, the visibility detection performance of the method proposed in this study may be reduced when dealing with complex scenes and extreme weather conditions. This provides room for improvement and optimization for future research.

5 Conclusion

HPVD is an important topic in the traffic safety, which is crucial for improving driving safety. The study constructed an HPVD by integrating Hough and IPNN, combining their advantages. These results confirmed that the average time taken for a video frame of 960×720 was 13.9 s, and the detection error between 500 and 1000 meters was 10.03%. The distribution of the minimum and maximum visibility values on the road surface during the day and evening was [183.57 m, 1183.26 m], while in the evening it was [139.58 m, 519.22 m]. Compared with traditional methods, the constructed HPVD can more accurately detect the visibility of road surfaces by comparing it with instrument detection values and true visibility values. The experiment verified the effectiveness and feasibility of this method, providing new ideas and methods for further research on HPVD. The research on visibility detection technology for highway engineering by Hough algorithm combined with IPNN involves several key fields and has a wide range of application prospects. In the highway engineering industry, it can provide real-time accurate visibility data for highway safety, accident prevention and traffic flow management. It not only promotes the development of related industries, but also brings a new development direction for visibility detection in highway engineering.

References

[1] Mingxu Liu, Ao Sun, Zelong Ni, Pengcheng Wang, and Enyu Bai. Highway visibility prediction model based on dark channel prior theory. Academic journal of computing and information science, 4(6):43-47, 2021. https://doi.org/10.25236/AJCIS.2021.040607

[2] Xiyu Mu, Qi Xu, Qiang Zhang, Junch Ren, Hongbin Wang, and Linyi Zhou. A combined multi-mode visibility detection algorithm based on convolutional neural network. Journal of signal processing systems, 95(1):49-56, 2023. https://doi.org/10.1007/s11265-022-01792-1

[3] Md Nasim Khan, and Mohamed M. Ahmed. Development of a novel convolutional neural network architecture named RoadweatherNet for trajectory-level weather detection using SHRP2 naturalistic driving data. Transportation research record, 2675(9):1016-1030, 2021. https://doi.org/10.1177/03611981211005470

[4] Min Wang, and Shudao Zhou. An adaptive visibility detection method based on a UAV-borne real-time panoramic camera. Journal of coastal research, 99(4):282-288, 2020. https://doi.org/10.2112/SI99-040.1

[5] Hongshuai Qin, and Huibin Qin. An end-to-end traffic visibility regression algorithm. IEEE, 10(5):25448-25454, 2021. https://doi.org/10.1109/ACCESS.2021.3101323

[6] Joy Purohit, and Rushit Dave. Leveraging deep learning techniques to obtain efficacious segmentation results. Archives of advanced engineering science, 1(1):11-26, 2023. https://doi.org/10.47852/bonviewAAES32021220

[7] Ying Meng, and Hongtao Wu. Highway visibility detection method based on surveillance video. 2019 IEEE 4th international conference on image, vision and computing (ICIVC), 13(5):197-202, 2019. https://doi.org/10.1109/ICIVC47709.2019.8981058

[8] Yang Ma, Yubing Zheng, Jianchuan Cheng, and Yunlong Zhang. Hybrid model for realistic and efficient estimation of highway sight distance using airborne LiDAR data. Journal of computing in civil engineering, 33(6):19-39, 2019. https://doi.org/10.1061/(ASCE)CP.1943-5487.0000853

[9] Aditi, and Ashrit Raghavendra. Assessment of forecast skill of high-and coarse-resolution numerical weather prediction models in predicting visibility/fog over Delhi, India. Current science, 120(4):676-683, 2021. https://doi.org/10.18520/cs/v120/i4/676-683

[10] Heng Ding, Yajie Cheng, Xiaoyan Zheng, Wenjuan Huang, Jiye Li, and Hanyu Yuan. Speed guidance and trajectory optimization of traffic flow in a low-visibility zone of a highway segment within multiple signalized intersections. Journal of advanced transportation, 2021:5579796, 2021. https://doi.org/10.1155/2021/5579796

[11] Yang Ma, Said Easa, Jianchuan Cheng, and Bin Yu. Automatic framework for detecting obstacles restricting 3D highway sight distance using mobile laser scanning data. Journal of computing in civil engineering, 35(4):4021008.1-4021008.19, 2021. https://doi.org/10.1061/(ASCE)CP.1943-

5487.00009

[12] M. S. Ismail, J. Purbolaksono, N. Muhammad, A. Andriyana, and H. L. Liew. Statistical analysis of imperfection effect on cylindrical buckling response. Materials science and engineering, 100(1):18-19, 2015. https://doi.org/10.1088/1757-899X/100/1/012003

[13] Said Easa, Yang Ma, Ashraf Elshorbagy, Ahmed Shaker, Songnian Li, and Shriniwas Arkatkar. Visibility-based technologies and methodologies for autonomous driving. Self-driving vehicles and enabling technologies, 11(9):1-25, 2020. https://doi.org/10.5772/intechopen.95328

[14] Sanmitra Banerjee, Mahdi Nikdast, and Krishnendu Chakrabarty. Characterizing coherent integrated photonic neural networks under imperfections. Journal of lightwave technology, 41(5):1464-1479, 2022. https://doi.org/10.1109/JLT.2022.3193658

[15] Xiaowei Shi, Dongfang Zhao, Handong Yao, Xiaopeng Li, David K. Hale, and Amir Ghiasi. Video-based trajectory extraction with deep learning for High-Granularity Highway Simulation (HIGH-SIM). Communications in transportation research, 1(1):100014, 2021. https://doi.org/10.1016/j.commtr.2021.100014

[16] Min Wang, Shudao Zhou, Zhanhua Liu, and Yangchun Zhang. Error analysis and improved design of target board reflection for visibility measurement by the image method. Journal of atmospheric and oceanic technology, 37(12):2299-2305, 2020. https://doi.org/10.1175/JTECH-D-20-0057.1

[17] Sahar Malmir, and Majid Shalchian. Design and FPGA implementation of dual-stage lane detection, based on Hough transform and localized stripe features. Microprocessors and microsystems, 64(11):12-22, 2019. https://doi.org/10.1016/j.micpro.2018.10.003

[18] Kourosh Kiani, Razieh Hemmatpour, and R. Rastgoo, Automatic grayscale image colorization using a deep hybrid model. Journal of AI and data mining, 9(3):321-328, 2021. https://doi.org/10.22044/jadm.2021.9957.2131

[19] Jian Chen, Ming Yan, Muhammad Rabea Hanzla Qureshi, and Keke Geng. Estimating the visibility in foggy weather based on meteorological and video data: A recurrent neural network approach. IET signal processing, 17(1):1-12, 2023. https://doi.org/10.1049/sil2.12164

[20] Darko Babić, Dario Babić, Mario Fiolić, Arno Eichberger, and Zoltan Ferenc Magosi. A comparison of lane marking detection quality and view range between daytime and night-time conditions by machine vision. Energies, 14(15):4666, 2021. https://doi.org/10.3390/en14154666

[21] Mingyuan Sun, Haochun Zhang, Ziliang Huang, Yueqi Luo, and Yiyi Li. Road infrared target detection with I-YOLO. IET image processing, 16(1):92-101, 2022. https://doi.org/10.1049/ipr2.12331